IOSR Journal of Applied Physics (IOSR-JAP)
e-ISSN: 2278-4861.Volume 8, Issue 5 Ver. III (Sep - Oct. 2016), PP 85-88
www.iosrjournals.org

Synthesis and structural properties of Zn1-xCrxO nanoparticles

H. A. Vardukar*
Department of Physics, Dayanand Science College, Latur - 413 512, Maharashtra, INDIA

***Abstract**: $Zn_{1-x}Cr_xO$ (x = 0.00, 0.05, 0.10) nanoparticles were synthesized by novel co-precipitation method. The synthesized samples are characterized by powder x-ray diffraction (XRD). The x-ray diffraction pattern confirms that doping of Cr did not change the ZnO hexagonal wurtzite structure. The Cr doped ZnO nanoparticles have average crystallite size in the range of 19 - 27 nm. The increase in lattice parameters with increasing Cr doping%, it confirmed that the Cr substitution in Zn-O lattice. The Cr doping increased the volume in ZnO nanoparticles which led to increase the bond length. The micro-strain also varied by depend the size of the nanoparticles. The stress was changed with respect to both compositional and size effects. The stress was increased with increasing Cr doping%, it noticed Cr^{2+} ion incorporation in ZnO host structure.*

***Keywords:** Chemical synthesis; X-ray diffraction; bond length; strain; stress.*

I. Introduction

Semiconductor nanoparticles have attracted much attention over the past few years because of their novel structural, optical and electrical properties originating from quantum confinement. The emphasis has been mainly placed on the synthesis of semiconductor particles belonging to II-VI and III-V groups, which show significant quantum confinement effects. Semiconductor nanoparticles exhibit size-dependent electronic band gap energies [1], melting temperatures [2] , solid-solid phase transition temperatures [3] and pressures [4]. In addition to these, doped semiconductor nanoparticles have tremendous potential application such as light emitting diodes. These properties of nanocrystals make them an interesting category of materials for optoelectronic applications. For example, ZnO is an important material and has a variety of applications such as catalysis, solar cells and other optoelectronic devices. Most transition metals doped ZnO samples are grown employing complex and expensive techniques like molecular beam epitaxy metal organic vapour phase epitaxy or pulsed laser deposition that require high grown temperatures, thermal hydrolysis technique [5], spray pyrolysis [6], chemical vapour deposition [7], thermal evaporation of Zn [8], hydrothermal syntheses [9, 10], low temperature wet-chemical reaction [11].The mean magnitude of the micro-strain and stress in nanocrystalline samples could be estimated from the X-ray diffraction pattern using different analytical procedures. This article reports a study of micro-strain in nanocrystalline $Zn_{1-x}Cr_xO$ particles from the X-ray diffraction pattern However; most of these preparation methods involve a strictly controlled synthesis environment, expensive equipment and complicated procedures. We have preferred co precipitation route for the synthesis of nanocrystalline $Zn_{1-x}Cr_xO$ particles because, it is a simple, fast and low cost effective method.

II. Experimental details

For synthesis of pure and Cr doped ZnO nanoparticles, the zinc acetate dehydrate (99.99% purity) $Zn(CH_3COO)_2.2H_2O$, Chromium nitrate (99.99% purity) $Cr(NH_3COO)_2.6H_2O$, sodium hydroxide NaOH, Methanol, Ethanol were purchased from Sigma Merck Limited, India. All chemicals were of analytical reagent grade (AR) and were directly used without any special treatment. Samples with compositional formula of $Zn_{1-x}Cr_xO$, with x = 0.00, 0.05 and 0.10 were prepared by co-precipitation route in an alcoholic medium (methanol). In this procedure, to prepare pure ZnO, Zinc acetate dehydrate was dissolved in methanol (100 ml) and other containing of NaOH in methanol (100 ml) were prepared and added both by constant magnetic stirring while heating at 285 K for 2 h. The precipitate separated from the solution by filtration, washed several times with distilled water and ethanol then dried in air at 400 K to obtain ZnO nanoparticles. The samples obtained were annealed at 683 K in air for 8 h. For the synthesis of Cr doped ZnO nanoparticles, Zinc acetate dehydrate and Chromium nitrate were dissolved in methanol (100 ml) and other containing of NaOH in methanol (100 ml) were prepared and added by constant magnetic stirring while heating at 285 K for 2 h. The precipitate separated from the solution by filtration, washed several times with distilled water and ethanol then dried in air at 400 K to obtain Cr doped ZnO nanoparticles. The samples obtained were annealed in air for 8 h at 683 K. A similar procedure for the synthesis of all varying contents of Cr doped ZnO (0-10%Cr doping) nanoparticles.

The prepared pure and Cr doped ZnO nanoparticles were characterized by XRD and TEM. The crystalline structure, phase purity and size of the nanoparticles were determined by X-ray diffraction (XRD) X-ray diffractometer (Model: PW-3710) employing Cuk_a (λ =1.5406 A°) radiation. It was used for recording X-ray diffraction pattern operating at 40 kV and 40 mA. The XRD patterns were recorded in the 26 range 20-80° with a scanning step of 0.02° and analyzed by comparing with the standard JCPDS cards.

III. Result and Discussion

3.1 Crystal structure: Lattice parameters

Fig 1. Show the X-ray diffraction patterns of $Zn_{1-x}Cr_xO$ samples with concentration X= 0.0, 0.05, 0.10 sintered at 400 °C. An increment in the diffraction intensity peaks with risings doping shown in Fig. 1. This shows that the crystallinity of the samples enhance with higher Cr doping.

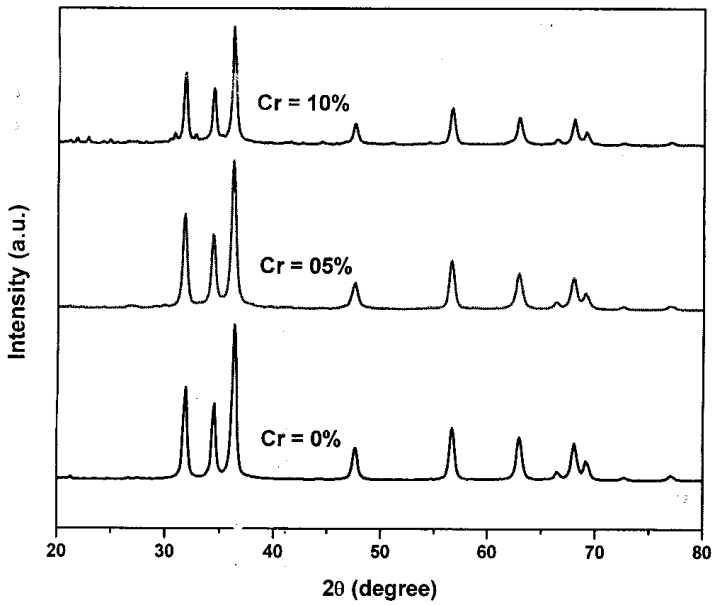

Figure 1. XRD pattern of Pure ZnO and Cr-doped ZnO nanoparticles of varying Cr dopant concentration.

The wurtzite lattice parameters 'a' and 'c' were calculated using the equation-

$$\frac{1}{d_{hkl}^2} = \frac{4}{3}\left[\frac{h^2 + hk + k^2}{a^2}\right] + \frac{l^2}{c^2} \qquad \ldots\ldots\ldots \quad (1)$$

Where d_{hki} is the interplanar spacing distance. The lattice parameters 'a' and 'c' of wurtzite structure increase with increasing concentration. It may be due to the larger ionic radius of Cr^{2+} ions as compared to Zn^{2+} ions. This indicates that the Cr^{2+} ions homogenously substitute for the Zn^{2+} ions in wurtzite structure. Lattice parameter values are close to those of lattice constant of a = 0.32488 nm & c = 0.52066 nm in the stranded data (JCPDS: 36-1451). The values of lattice parameters are summarized in table 1. The unit cell volume is calculated for all samples using lattice parameters. It indicates that the values of the unit cell volume are increasing with increasing Cr concentration. The enhancement in values of the unit cell volume may be due to the ionic radii in agreement with the linear Vegard's laws. The increment of lattice parameters with increasing Cr content shows that the Cr^{2+} (*0.087* nm) [12] ions replace Zn^{2+} *(0.074* nm) ions to occupy the 2b crystallographic site since, the ionic radii of Zn^{2+} ions aresmaller than the ionic radii of Cr ions. The volume cell goes on increasing with increasing Cr content.

The value of lattice parameters were decreases with increasing Cr doping in ZnO nanoparticles reported [13-15]. But first time, we report on experimental evidences that there is no formation of secondary phases or extra impurity phases and increasing the lattice parameters a & c even upto 10 % Cr doping in ZnO. It persists wurtzite structure even upto 10% Cr doping owing to Cr clustering and not due to formation of secondary phases or extra impurity phases.The average crystallite size of the nanoparticles is calculated after appropriate background correction from X- ray line broadening of the diffraction peaks of (101) plane using Debye Scherrer's formula [16],

$$D = \frac{K\lambda}{\beta_{hkl} Cos\theta} \qquad \ldots\ldots\ldots (2)$$

Where D = crystalline size, K= shape factor (0.9), λ = wavelength of Cuk_α radiation, instrumental corrected integral breadth of the reflection (in radians) located at 2θ and θ = angle of reflection (in degree) was utilized to relate the crystalline size of the line broadening. From the calculations, the average crystalline sizes of the Pure and Cr doped ZnO nanoparticles are in the range of 14 - 19 nm. The crystalline sizes of ZnO nanoparticles are varying

with increasing Cr concentration, these values are summarized in table 1.

Table 1: Lattice parameters, volume & average crystallite size of Cr doped ZnO nanoparticles.

Samples	Lattice parameters		Volume $(Å)^3$	Average crystallite size (nm)
	a (Å)	c (Å)		
Pure ZnO	3. 243402	5.192577	47. 3045	18.50491
5%	3. 253303	5. 221755	47. 86119	16. 80042
10%	3. 255302	5. 223231	47. 93357	14. 95457

3.2 Crystal structural: parameter u, bond length, micro-strain, stress

The doping of Cr is increased in ZnO crystal a significant decrease in c/a ratio. The u parameter is calculated using following formula

$$u = \frac{a^2}{3c^2} + 0.25 \quad \text{…….(3)}$$

The values of u parameter are almost constant and increasing of Cr doping in ZnO host materials the u parameter is increased. This suggests that Cr is able to substitute in ZnO crystal. The changing lattice parameters, volume of unit cell, u parameters and bond length are shown in table 1. The effect of Cr doping on Zn-O bond length (L) are calculated using following formula

$$L = \sqrt{\frac{a^2}{3} + \left(\frac{1}{2} - u\right)^2 c^2} \qquad \text{…….(4)}$$

In generally, increase in Zn-O bond length is observed with respective to increase in Cr doping. It indicates that Cr doping in ZnO without changing the hexagonal wurtzite crystal structure. The Zn-O bond length calculated is 1.97746 $\overset{0}{A}$; whereas the reported Zn-O bond length in the unit cell of ZnO and neighboring atoms is 1.9767 $\overset{0}{A}$ [17]. The calculated bond length agrees with the Zn-O bond length in the unit cell.

The strain induced in powders due to crystal imperfection and distortion was calculated using the formula

$$\varepsilon = \frac{\beta_{hkl}}{4\tan\theta} \quad \text{……. (5)}$$

The micro-strain increases with increasing Cr doping in ZnO nanoparticles and tabulated in table2.

The stress (σ) in the ZnO plans can be determined using the following expression [18],

$$\sigma = -233\times10^9\left(\left(C_{bulk} - C\right)/C_{bulk}\right) \quad \text{…… (6)}$$

where C is the lattice constant of ZnO planes calculated from x-ray diffraction data, C_{bulk} is the strain-free lattice parameter of ZnO (5.1916 $\overset{0}{A}$). The compressive stress increased with increasing Cr introduction in Zn - O lattice and the subsequent strain increases the compression along c-axis. The increased compression along c-axis is due to the increase of lattice volume and bond length.

Table 2: u parameter, bond length, strain & stress of Cr doped ZnO nanoparticles.

Samples	u parameter	Bond Length L	Strain	Stress (GPa)
Pure ZnO	0.380051	1.973445	0.00201	0.043854
5%	0.379388	1.981073	0.002242	1.353369
10%	0.379388	1.982081	0.002511	1.419621

Morphological Study :-

The morphology and structural characteristics were investigated by TEM. The images of pure ZnO sample and 5%, 10%, Cr doped ZnO are as shown in the Figure 2(a-c). It can be seen that all the samples are spherically shaped with narrow size distribution. The average particle size prepared samples are in the range of 19 – 27 nm. This small size of particle detected using TEM are in agreement with XRD result. All though we cannot exactly determine the Cr concentration by this method but it shows the existence of Cr ion Cr^{+2} in Cr doped ZnO. It is observed that there are large amount of Cr doped ZnO nanoparticles. It shows uniform distribution of dopant throughout the sample.

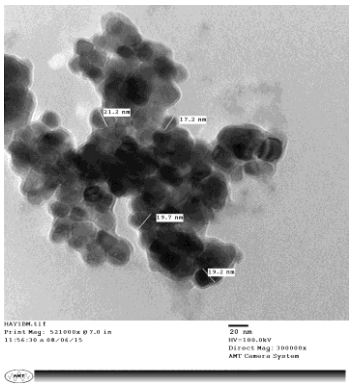

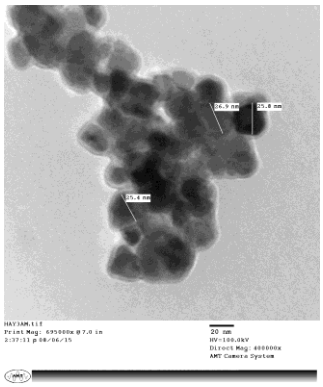

Figure 2(a). TEM image of ZnO sample. **Figure 2(a).** TEM image of 5% Cr doped ZnO sample.

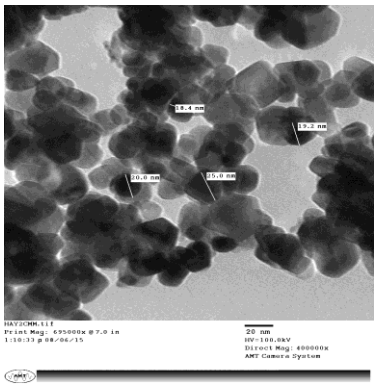

Figure 2(c). TEM image of 10% Cr doped ZnO sample.

IV. Conclusion

The samples of pure and Cr doped ZnO nanoparticles were synthesized by co-precipitation route. The nanocrystalline Cr doped ZnO samples have wurtzite (hexagonal) structure and single phase ZnO without any impurity phases. It shows that substitution of Cr ions in ZnO without changing the wurtzite structure upto x = 10%. The lattice parameters are increased with increasing the Cr concentration of the samples, it may be due to the larger ionic radius of $Cr\,2^{+}$ ions. The average crystallite size of the prepared pure and Cr doped ZnO nanoparticles in the range 19 - 27 nm. The value of volume was increasing trend with increase Cr doping %. The parameter u represents the relative position of the anion sub-lattice. The values of u parameter are close to ideal value of u parameter and enhancement u means a softer Zn-O bond along the c-axis direction. The micro-strain and stress were enhanced with increasing Cr doping concentration.

References

[1]. L. E. Brus, *J. Chem. Phys.* **80**, 4403 (1984) A. N. Goldstein, C. M. Echer and A. P. Alivisatos, *Science* **356**, 1425 (1992)
[2]. S. B. Qadri, E. F. Skelton, D. Hsu, A. D. Dinsmore, J. Yang, H. F. Gray and B. R. Ratna *Phys. Rev.* B **60**, 9191 (1999)
[3]. C. C. Chen, A. B. Herhold, C. S. Johnson and A. P. Alivisatos, *Science* **276**, 398 (1997)_ H. K. Park, D. K. Kim, C. H. Kim, J. Am. Ceram. Soc. **80**, 743 (1992). T. T. Kodas, Adv. Mater. **6**, 180 (1989).
[4]. B. P. Zhang, N. Y. Binh, K. Wakatsuki, Y. Segawa, Y. Yamada, N. Usami, M. Kawasaki, H. Koinuma, J. Phys. Chem. B **108**, 10899 (2004).
[5]. G. Z. Shen, Y. Bando, Ch.J. Lee, J. Phys. Chem. B **109**, 10578 (2005).
[6]. S. I. Hirano, Ceram. Bull. **66**, 1342 (1987).
[7]. H. Zhang, D. R. Yang, D. S. Li, X. Y. Ma, S. Z. Li, D. L. Que, Cryst. Growth Des.2, 547 (2005).
[8]. B. Liu, H.C. Zeng, Langmuir **20**, 4196 (2004). http://en.wikipedia.org/wiki/Ionic_radius L.B. Duan · X.R. Zhao · J.M. Liu · T. Wang · G.H. Rao, ApplPhys A, 99, 679-683 (2010).
[9]. C. F. Fu, L. F. Han, C. Liu, and Y. F. Gaol Phys. Status Solidi A, (2013) 1-5/ DOI 10.1002/pssa.201329014.
[10]. S. Safa, A. MasoudiNejad, Journal of Advanced Materials and Processing, Vol.2, No. 1, 19-24,2014.
[11]. S. Muthukumaran, R. Gopalakrishnan, Optical Mater. 34, 1946-1953 (2012).
[12]. Seetawan, U., Jugsujinda, S., Seetawan, T., Ratchasin, A., Euvananont, C., Junin, C., Thanachayanont, C., Chainaronk, P. Maters. Sci. Appls. 2, 1302-1306 (2012).